



Available online at [www.sciencedirect.com](http://www.sciencedirect.com)



International Journal of Pharmaceutics 280 (2004) 185–198

international  
journal of  
pharmaceutics

[www.elsevier.com/locate/ijpharm](http://www.elsevier.com/locate/ijpharm)

## AFM studies of the crystallization and habit modification of an excipient material, adipic acid

T.R. Keel, C. Thompson<sup>1</sup>, M.C. Davies, S.J.B. Tendler, C.J. Roberts\*

*Laboratory of Biophysics and Surface Analysis, School of Pharmacy, The University of Nottingham,  
University Park, Nottingham NG7 2RD, UK*

Received 16 December 2003; received in revised form 10 May 2004; accepted 20 May 2004

### Abstract

Atomic force microscopy (AFM) has been used to investigate the (100) face of crystalline adipic acid, both in air and liquid environments. In air, surface reorganization occurred during scanning of the AFM probe, which has been investigated using single point force–distance analysis under a controlled relative humidity (RH) environment. We suggest such reorganization can be attributed to the influence of a network of water molecules bound to the hydrophilic (100) surface permitting local AFM tip-enhanced dissolution and reorganization of the solute. *In situ* imaging was also carried out on the crystals, revealing etch-pit formation during dissolution, and rapid growth at higher levels of supersaturation ( $\sigma$ ), both of which are direct consequences of the hydrophilic nature of the (100) face. Also presented here are nanoscale observations of the effect of octanoic acid, a structurally-related habit modifier, on crystalline adipic acid. Using AFM, we have been able to show that the presence of octanoic acid at low concentration has little observable affect on the development of the (100) face; however, as this concentration is increased, there are clear changes in step morphology and growth mode on the (100) face of the crystal. At a concentration of 1.26 mmol dm<sup>-3</sup> (a concentration corresponding to a molar ratio of approximately 1:175 octanoic acid:adipic acid), growth on the (100) face is inhibited, with *in situ* AFM imaging indicating this is a direct consequence of octanoic acid binding to the surface, and pinning the monomolecular growth steps.

© 2004 Elsevier B.V. All rights reserved.

**Keywords:** Atomic force microscopy (AFM); Crystallization; Habit modification; Solute reorganization; Etch pit formation

### 1. Introduction

The physical properties of the solid state of both drugs and excipients are of considerable importance in the pharmaceutical industry as they can effect both the production of effective and safe dosage forms, and

the biological behaviour of the finished form (Florence and Attwood, 1988).

Crystallization plays a vital role in a number of stages in the production of pharmaceutical materials. Initially, purification and separation define a material's chemical purity and physical properties. Further downstream in the manufacturing process, crystal properties can influence a range of industrial formulation factors such as bioavailability, milling, tabletting, agglomeration and flow properties of powders.

The incorporation of guest molecules (impurities, additives or crystallizing solvent) into host crystals is

\* Corresponding author. Tel.: +44 115 9515048;  
fax: +44 115 9515110.

E-mail address: [clive.roberts@nottingham.ac.uk](mailto:clive.roberts@nottingham.ac.uk) (C.J. Roberts).

<sup>1</sup> Present address: Medway Sciences, University of Greenwich, Medway Campus, Chatham, Kent ME4 4TB, UK.

inevitable during crystallization from solution (Zhang and Grant, 1999). Generally it can be assumed that there is some form of affinity between an active impurity and the crystallizing species of interest. With organic molecules, affinity between the 'guest' and 'host' molecule often stems from a structural similarity, which has led to the use of the term 'tailored' crystal growth (Mullin, 2001).

Structurally-related molecules frequently act as impurities in molecular crystals. These substances may have been introduced to the crystallization medium for a specific purpose, or might be impurities resulting from the synthesis or degradation of the desired product. Thus, literature is replete with references to the additive-induced effects on crystalline drug compounds. Some of the reported additives are polymeric molecules that act as nucleation inhibitors, allowing the successful topical delivery of drugs in a super-saturated state (Davis and Hadgraft, 1991; Raghavan et al., 2000, 2001). Other reports concern the effect of small molecule inhibitors on the growth and dissolution of pharmaceutical compounds such as  $\alpha$ -lactose monohydrate (Garnier et al., 2002), paracetamol (Chow et al., 1985; Chow and Grant, 1988a,b; Hendriksen and Grant, 1995; Hendriksen et al., 1998) and salicylic acid (Wilkins et al., 2002).

However, probably the most widely studied of all pharmaceutically relevant small molecules is adipic acid, an excipient used as an acidulant in effervescent tablet formulations and as a tablet lubricant. The habit modification of crystalline adipic acid was first quantitatively observed in the presence of anionic and cationic surfactants (Michaels and Colville, 1960; Michaels and Tausch, 1961). However, it is the effect of a series of *n*-alkanoic acids on the crystal habit that has received most attention. Simple molecules such as caproic, heptanoic, octanoic and decanoic acids are structurally similar to adipic acid making such materials ideal to act as relevant habit modifiers. Numerous research papers have reported the severe habit modification observed in adipic acid crystals when doped with relatively low concentrations of alkanoic acids (Fairbrother and Grant, 1978, 1979; Davey et al., 1992) along with the effects of doping on dissolution rate, crystal energy and density, and melting point (Chow et al., 1984, 1986; Chan and Grant, 1989). Molecular modeling techniques have also been employed to calculate both the theoreti-

cal morphology of adipic acid crystals (Pfefer and Boistelle, 2000) and the binding energies present between various long chain alkanoic acids (octanoic acid and above) and the (100) face of adipic acid (Myerson and Jang, 1995).

The primary aim of this report is to visualize at the nanoscale the (100) face of both un-doped adipic acid crystals, and crystals grown in the presence of octanoic acid. This has been achieved using atomic force microscopy (AFM). We have previously employed AFM to visualize the dissolution of aspirin (Danesh et al., 2001) and the growth of paracetamol crystals (Thompson et al., 2004). Here our studies have revealed an apparent surface restructuring in air of the adipic acid crystal lattice under typical AFM imaging conditions, a phenomenon ascribed to local dissolution and reorganization of the solute. *In situ* imaging also reveals the growth and dissolution behaviour of adipic acid crystals, both in the presence and absence of the structurally-related habit modifier, octanoic acid.

## 2. Materials and methods

### 2.1. Materials

Adipic acid and octanoic acid were both purchased from Sigma-Aldrich (Sigma-Aldrich, Gillingham, UK) and used as received. The solvent used throughout was HPLC grade water (18.2 M $\Omega$  cm resistivity).

### 2.2. Growth of seed crystals

A series of experiments were carried out to identify conditions to grow suitably large (>1 mm), well-faceted seed crystals for AFM experiments. The optimized protocol was as follows. 2.05 g of adipic acid was added to 200 ml of water and dissolved by sonication. The resulting undersaturated solution was filtered and placed in the refrigerator at 4 °C. Generally, after 72 h suitably sized crystals had nucleated and grown. Such crystals were then rapidly vacuum filtered, washed and dried lightly with absorbent tissue paper. The crystals were subsequently dried overnight in an oven at 60 °C and stored in a desiccator until required.

Adipic acid crystallizes in the monoclinic crystal system and has the space group *P*2<sub>1</sub>/*c*, with two

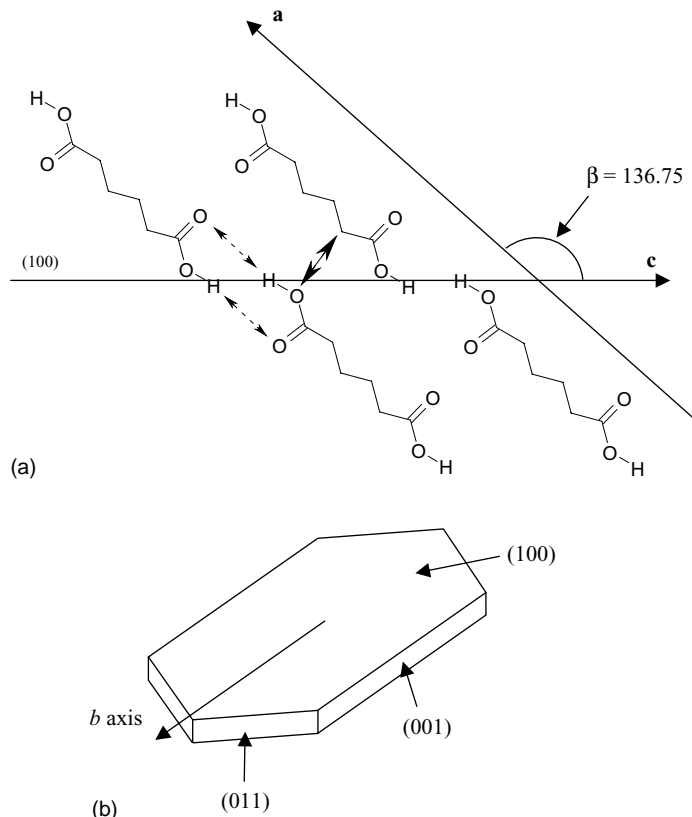


Fig. 1. (a) A schematic illustrating the structure of crystalline adipic acid, as viewed down the *b* axis. The hydrogen bonding and van der Waals interactions present are highlighted with dotted and bold arrows, respectively. (b) The experimental morphology of a typical crystal grown from aqueous solution.

molecules per unit cell. The unit cell parameters are  $a = 10.01 \text{ \AA}$ ,  $b = 5.15 \text{ \AA}$  and  $c = 10.06 \text{ \AA}$ , with  $\beta = 136.7$  (Housty and Hospital, 1965). The structure of the adipic acid crystal, along with a schematic illustration of the experimental morphology of adipic acid crystals grown from water, is presented in Fig. 1.

### 2.3. Preparation of imaging solutions

The relative supersaturation of all imaging solutions was calculated using Eq. (1):

$$\sigma = \ln \left( \frac{c}{c_0} \right) \quad (1)$$

where  $c_0$  is the solubility of adipic acid at a given temperature, and  $c$  is the concentration of adipic acid dis-

solved in the solvent (water). Solubility data for this system is provided in Fig. 2, and is in the form of a polynomial fit of adipic acid solubility in water versus temperature (Fairbrother, 1981). All AFM experiments were carried out at room temperature (25 °C).

However, it must be noted that the temperature within the AFM liquid cell is slightly elevated when compared to the room temperature due to the heat generated by the AFM piezoelectrics and laser light (Kipp et al., 1995). Inevitably, this raises the solubility of adipic acid (see Fig. 2), causing the calculated values of supersaturation to be artificially high. This explains why, for example, dissolution was observed in an apparently supersaturated solution (Section 3.2). This effect is difficult to quantify, especially when dealing with a material such as adipic acid whose solubility is highly dependant on temper-

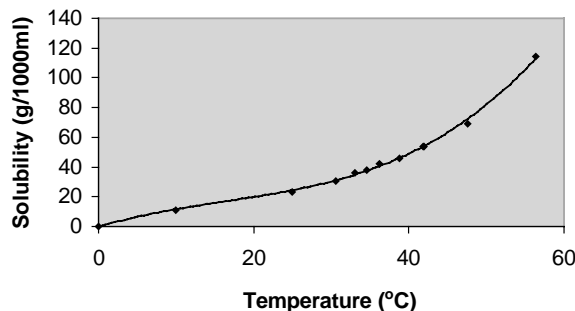


Fig. 2. Solubility of adipic acid in water, as a function of temperature. Adapted from Fairbrother (1981).

ature. As such, the values of supersaturation quoted throughout have been calculated using the solubility of adipic acid in water at 25 °C (23.45 g/1000 ml), and are accurate relative to one another at this temperature.

The following protocol was utilized to make up the imaging media. The calculated quantity of adipic acid was dissolved in 5 ml of water by stirring at 238 rpm, at 50 °C. If the solution was to contain a habit modifier, the desired quantity was added at this point. The solution was stirred for approximately 60 min to ensure complete dissolution, after which it was filtered and left to cool to 25 °C prior to being introduced into the AFM liquid cell. All values of supersaturation and quantities of habit modifier will be quoted and discussed in Section 3.

#### 2.4. AFM analysis

Well faceted crystals (diameter >1 mm) were selected for AFM analysis by optical microscopy. Once a suitable crystal had been identified, it was mounted on a 10-mm glass coverslip (Agar Scientific, Stansted, UK) using Tempfix (Agar Scientific), which in turn was fixed to a magnetic AFM stub. Being the crystal face of interest during the present study, the (100) face was mounted parallel to the coverslip.

All images were recorded using a DI multimode atomic force microscope equipped with a Nanoscope IIIa controller (Veeco, Santa Barbara, CA). Silicon nitride NP-S cantilevers with a nominal spring constant of 0.1 N m<sup>-1</sup> were used throughout (Veeco). The DI multimode was equipped with an E-scanner with a

maximum scan size of 13 μm × 13 μm. Images were collected in both tapping and contact mode, using a minimum contact force at all times to avoid damaging the crystal face. All images were collected at either 256 × 256 or 512 × 512 pixel resolution, at a scan rate in the range of 2–8 Hz.

Experiments carried out in solution utilized a liquid cell (Veeco), equipped with a small o-ring to prevent solvent evaporation. Prior to each experiment in liquid the selected crystal was imaged in air to ensure the tip was of good quality and the area of crystal to be investigated was representative of a typical adipic acid crystal.

The images presented throughout this study are in the form of either topography or deflection data. Topography micrographs are constructed from the movement of the z-piezo in response to the AFM controller feedback system, and contain accurate three-dimensional data. The deflection images are constructed directly from the movement of the laser on the AFM photodiode. These images often highlight rapid changes in topography in greater detail, such as is seen at step edges, and are used for that purpose throughout this report.

Force–distance data presented herein were also collected using the DI multimode AFM. This data comes in the form of tip approach–retract curves, which can provide quantitative information of forces present between the tip and sample of interest as a function of tip–sample distance.

The same cantilever, which was initially cleaned in weak argon plasma for 5 s, was used throughout the single point force–distance experiments, allowing direct comparison of data. Curves presented are corrected from deflection versus piezo deflection, to true force (nN) versus probe-sample separation data.

#### 2.5. Scanning electron microscopy (SEM) analysis

All samples were gold coated using a Balzers SCD 030 Sputter Coater (Balzers Union Limited, Liechtenstein), operated at 0.1 mbar with a sputtering current of 30 mA. The duration of coating was 4 min. A Philips 505 SEM (Philips Electron Optics, Eindhoven, The Netherlands) was used to image all samples under a range of magnification settings at a voltage of 23 keV, with a spot size of 50 nm.

### 3. Results and discussion

#### 3.1. Surface restructuring on the (100) face of un-doped adipic acid crystals

To our knowledge, no AFM studies have previously been carried out on crystalline adipic acid, so initial experiments were carried out in air in an attempt to characterize the (100) face of the crystal. A typical AFM topography image is shown in Fig. 3. As expected, the surfaces of the crystals are dominated by step edges that have been pinned by foreign particles adsorbed on the crystal surface (Cabrera and Vermilyea, 1958). The single-molecule steps were consistently around 0.7 nm in height ( $\pm 0.15$  nm), a figure that is directly comparable to 0.685 nm, the interplanar distance normal to the (100) face deduced from crystallographic studies (Housty and Hospital, 1965).

On a number of separate occasions during the preliminary characterization experiments presented here, an apparent reorganization of adipic acid on the surface of the crystal was observed. Fig. 4 shows four consecutive tapping mode images. These images illustrate a clear change in surface morphology in a short space of time. Solute is clearly nucleating on the step terraces in Fig. 4b, and subsequently being in-

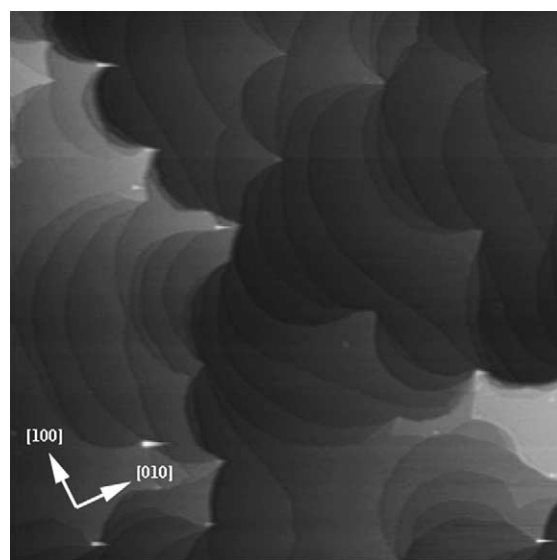


Fig. 3.  $10\text{ }\mu\text{m} \times 10\text{ }\mu\text{m}$  topographical AFM image of the (100) face of a typical un-doped adipic acid seed crystal.  $z$ -range, 35 nm.

corporated into the advancing monomolecular steps in Fig. 4c.

To our knowledge, such solute reorganization has only previously been observed on crystals of cadmium mercury thiocyanate (CMTc), a nonlinear optical material (Jiang et al., 2001, 2002a,b). These reports detailed a variety of phase transitions and surface morphology transformations, including the transformation of amorphous aggregates to microcrystals, and alteration of step shapes and defects. The authors attributed the apparent restructuring of the crystal surface to the inevitable increase in internal energy of the lattice after prolonged periods of contact mode imaging, which in turn promoted the gradual formation of increasingly stable states of the crystal.

Our observations are somewhat different to the report of Jiang et al. Reorganization has been observed after just a few minutes scanning in one area, in both contact (data not shown) and tapping mode. Tapping mode scanning negates many of the unfavourable probe–sample interactions associated with contact mode, and can lower lateral forces exerted on the sample surface to an almost negligible level, although contact forces can still be considerable at maximum loading. The observation of reorganization so rapidly after the onset of scanning indicates that, in addition to any tip–sample interaction, the surface chemistry of the crystal may be playing a significant part in the apparent solute mobility.

To further investigate these observations a series of single point force–distance experiments were carried out, the results of which are displayed in Fig. 5. Fig. 5a is characteristic of a typical force–distance curve acquired on a crystal of adipic acid in ambient air conditions ( $\text{RH} \sim 30\%$ ). The jump-to-contact on tip approach to the crystal surface is relatively small, whilst the jump-off-contact is considerably larger. Such a comparatively large adhesion is due to the meniscus force exerted by layers of water adsorbed on the sample surface. Indeed, when the crystal and the AFM tip were immersed in a saturated aqueous solution of adipic acid, the large capillary-induced adhesion force was negated (data not shown).

In the case of adipic acid, the presence of a significant meniscus force on the (100) face in ambient conditions is inevitable as it is constructed entirely of carboxylic groups (see Fig. 1). The hydrophilic nature of such groups is likely to induce strong at-

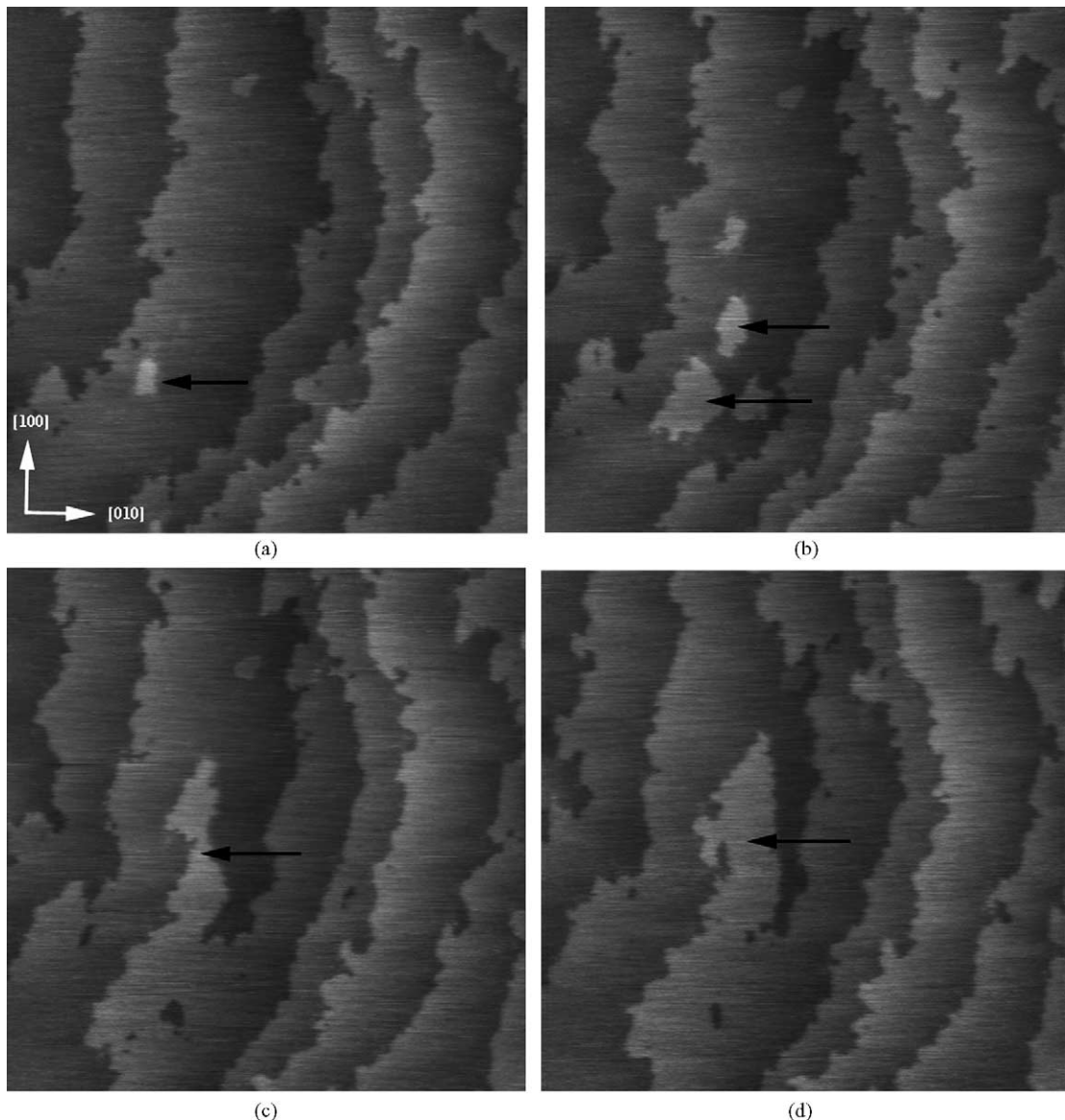


Fig. 4. Consecutive  $1.5 \mu\text{m} \times 1.5 \mu\text{m}$  tapping mode images of an adipic acid crystal, recorded in air at a scan speed of 3 Hz. Widespread solute reorganization on the crystal surface is clearly evident, some of which is highlighted by arrows.  $z$ -ranges of (a–d), 8 nm.

tractive forces between the sample surface and the thin water layer covering it. Theoretically, perturbation of this bound water layer by the raster motion of the tip may induce local dissolution and reorganization of the solute molecules on the crystal surface, giving rise to the effects observed during scanning.

In an attempt to further investigate the likelihood of dissolution and reorganization occurring on the crystal surface, force–distances curves were also carried out on the crystals in a 0% relative humidity (RH) environment and a typical curve is displayed in Fig. 5b (this curve has been translated 50 nm on the  $z$ -displacement axis for clarity). There have been

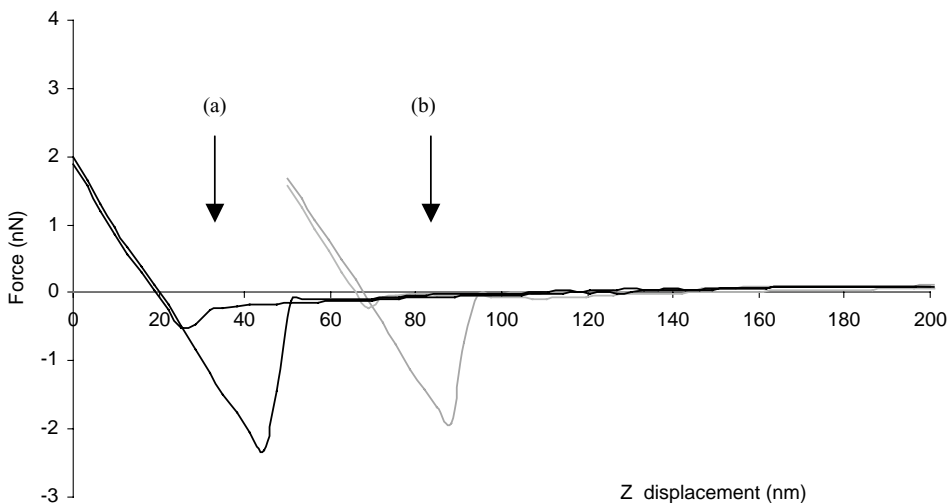


Fig. 5. Force–distance displacement data obtained from the (100) face at ambient (a) and low (b) relative humidity. Curve (b) has been translated 50 nm to the right for clarity.

numerous studies previously investigating the dependence of pull-off forces on RH, many of which have been covered in Cappella's comprehensive review article (Cappella and Dietler, 1999). Generally, as the RH is lowered toward 0%, the pull-off force decreases in magnitude due to the removal of lesser-bound water molecules at the sample surface. However, when comparing Fig. 5a and b there appears to be a negligible decrease in pull-off force when lowering the RH from ambient conditions of ~30% to 0%. This suggests that a significant layer of water is *strongly* adsorbed to the (100) surface. It seems feasible that such conditions, promoted by the interaction of the AFM tip on the surface, facilitate dissolution and re-organization of the solute within the bound 'network' of water molecules on the surface as observed in the sequence of images in Fig. 4.

The hydrophilic nature of the (100) face demonstrated here is of utmost importance in a number of aspects of the growth and morphology of adipic acid crystals. Theoretically, the formation of the (100) face should be rapid due to the hydrogen bonding which occurs between adipic acid chains to construct that face (see Fig. 1). In fact, it is the slowest growing of all the faces, which is the reason the crystal takes the shape of a thin plate rather than a needle-like morphology. The slow growth rate is generally believed to be due to adipic acid molecules effectively having to

compete with the occupying water molecules to bind at the crystal surface. This leads to a situation where desorption of the water molecules may play a significant role in determining the relative growth rate of the crystal faces (Davey et al., 1982, 1992).

### 3.2. Dissolution and growth of adipic acid crystals

As previously discussed, there have been numerous reports of the bulk dissolution and growth behaviour of crystalline adipic acid. One of the main advantages of AFM is the ability to perform experiments *in situ*, which allows data to be collected in real time under conditions directly relevant to the system of interest. In the case of adipic acid, *in situ* AFM allows the investigation of growth and dissolution of the (100) face of single crystals under controlled imaging media.

Initially, experiments were conducted to identify conditions suitable for such investigations. Imaging solutions with  $\sigma > 0.45$  promoted the spontaneous nucleation of microcrystals of adipic acid in the imaging solution, which rapidly coated the cantilever and sample surface, effectively prohibiting scanning. Conversely, at  $\sigma < 0.2$ , dissolution and etch pits became apparent on the seed crystal surface.

The formation of etch pits was in itself an interesting observation. Fig. 6a contains a typical light microscopy image of etch pits formed on the crystal

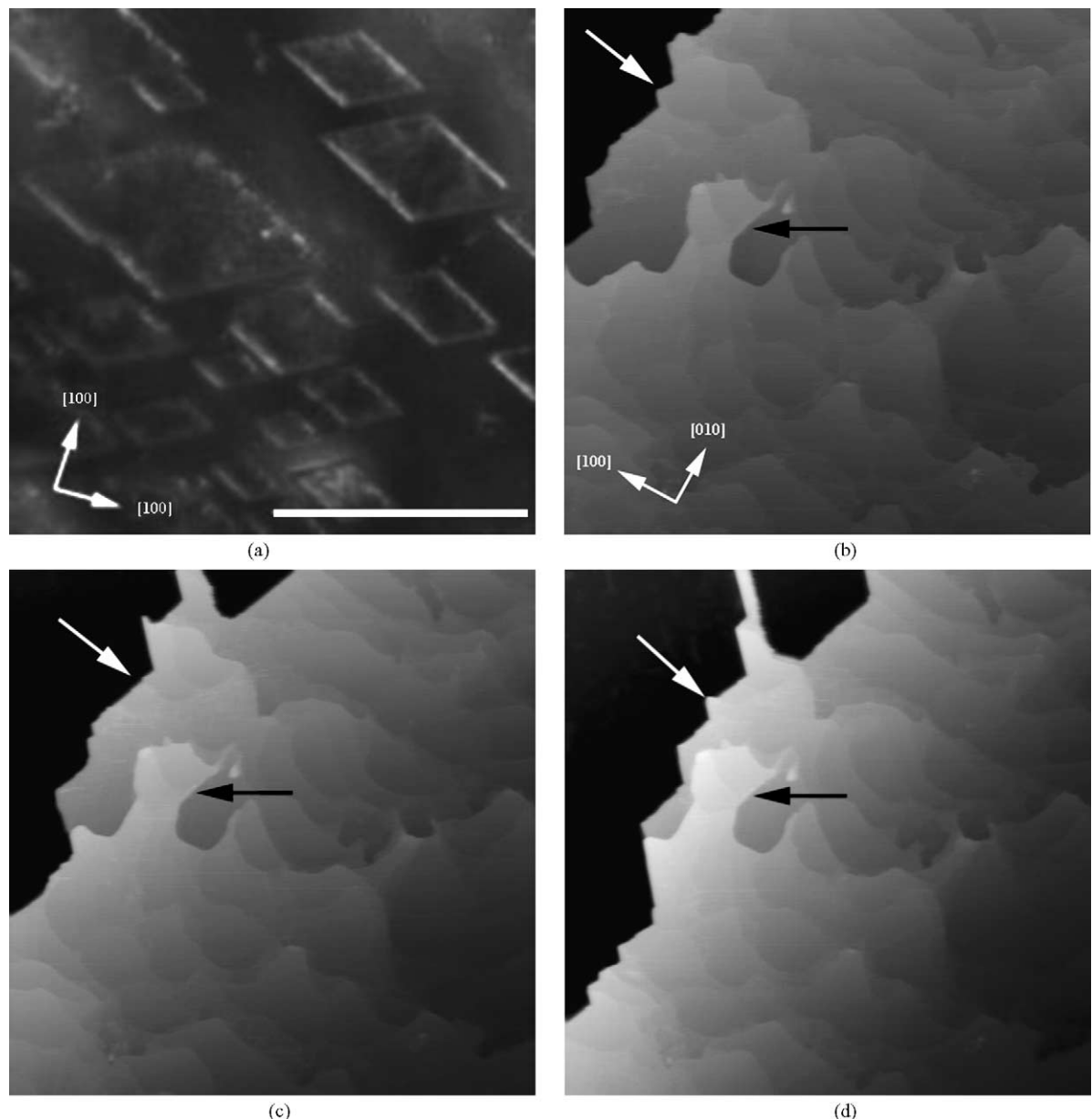


Fig. 6. Dissolution and etch-pit formation on un-doped adipic acid crystals. (a) Light microscope image of etch pits formed on the crystal surface. Scale bar, 50  $\mu$ m. (b–d) Consecutive 10  $\mu$ m  $\times$  10  $\mu$ m topography images illustrating selective dissolution on the crystal surface. The etch pit edge is approximately 150 nm in height, with dissolution proceeding from left to right as indicated by the white arrows. The terrace to the right of the advancing etch pit is not undergoing dissolution, an area of which is highlighted with black arrows.  $z$ -range, 200 nm in (b–d).

surface after being immersed for approximately 30 min in solution,  $\sigma = 0.15$ . It has been established that etch pits form at the site of an emergent dislocation (Shimon et al., 1985), and the etching only becomes apparent when the surface is ‘poisoned’ by an impurity. However, under the conditions created in these experiments, the only other substance present in the crystallization medium is the solvent, water. Indeed, the solvent–crystal interaction has previously been shown to affect the formation of etch pits on acetaminophen crystals, and plays an important role in the detachment and surface diffusion of surface molecules (Li et al., 2000).

As we have shown in Section 3.1, water is undoubtedly bound to the hydrophilic (1 0 0) surface and the presence of etch pits on this face may indicate that the bound water discourages dissolution by ‘poisoning’ the horizontal surfaces within and around a dislocation. However, the less hydrophilic surfaces initially exposed by dissolution at the emergent dislocation will not be protected by such tightly bound water molecules and dissolve more freely, leading to the formation of the observed pits.

To investigate this theory, *in situ* AFM was performed on a seed crystal at  $\sigma = 0.15$ , and images obtained shown in Fig. 6b–d. The large step ( $\sim 150$  nm in height) represents the edge of an etch pit, and is dissolving freely across the image from left to right. However, the terrace to the right of the widening etch-pit boundary is completely unchanged throughout imaging, with the smaller steps showing no indication of dissolution normal or parallel to the crystal surface. We believe this represents strong microscopical evidence of the ‘masking’ role played by the bound water to the hydrophilic (1 0 0) surface of crystalline adipic acid.

To encourage growth, the imaging medium had to be at a relatively high supersaturation, presumably to disrupt the bound water molecules at the surface. When this condition was met ( $\sigma > 0.3$ ) growth occurred rapidly, both tangentially and normally to the surface. A typical image obtained during such experiments is shown in Fig. 7. Large macrosteps, which always appeared to be the dominant growth mode, incorporate solute molecules in the highly unstable system and sweep rapidly across the crystal surface. However, growth always came to a halt quickly probably because vast quantities of solute were ‘lost’ to the

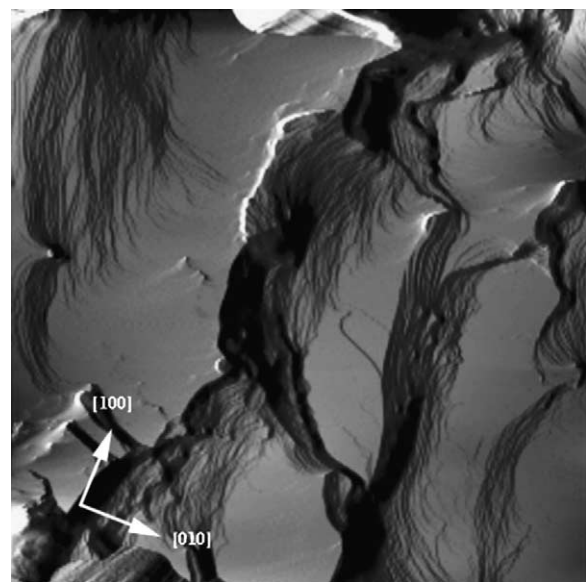


Fig. 7. A typical  $10 \mu\text{m} \times 10 \mu\text{m}$  deflection image captured during un-doped adipic acid growth, relative supersaturation = 0.4. The two large macrosteps running through the center of the image are approximately 300–400 nm in height.

crystal, forcing the relative supersaturation below the required threshold for growth to proceed. Presumably as the supersaturation fell below this value, significant quantities of water molecules were able to re-adsorb to the surface, and interfere with growth again.

### 3.3. Microscopical observations of the crystallization of adipic acid in the presence of the structurally-related habit modifier, octanoic acid

As previously discussed, the effect of the family of *n*-alkanoic acids on the crystallization of adipic acid has been the subject of numerous structural and kinetic studies (Fairbrother and Grant, 1978, 1979; Fairbrother, 1981; Davey et al., 1992; Williams-Seton et al., 2000). Crystals grown in the presence of small quantities of various *n*-alkanoic acids regularly display a range of characteristic morphological changes such as an elongation of the crystals along the *b*-axis, narrowing of the central region in the [1 0 0] zone and pronounced curvature of the faces.

Davey et al. (1992) found octanoic acid to be the most effective growth disrupter of the series of *n*-alkanoic acids due to its size—an eight carbon

chain causes maximum steric disruption to the (0 0 1) surface when incorporated into the growing face, subsequently preventing the next adipic acid molecule occupying its lattice site. Inevitably, this slows crystal growth, giving the (0 0 1) surface increased morphological importance. Williams-Seton et al. (2000) reported similar observations in the case of decanoic acid. However, these experimental studies also indicated that the growth of the (1 0 0) surface is largely unaffected by the presence of such structurally-related habit modifiers. This is generally believed to be another consequence of the hydrophilic nature of this face—presumably, the strongly adsorbed water layer is able to reject the majority of the hydrophobic alcanoic acid molecules. Consequently, the (1 0 0) surface is still morphologically dominant at low additive concentration.

In an attempt to microscopically assess this effect, we have performed both *in situ* and *ex situ* studies of the (1 0 0) face of adipic acid grown in the presence of the structurally-related habit modifier, octanoic acid.

Seed co-crystals were grown for *ex situ* AFM analysis in the presence of  $0.034 \text{ mmol dm}^{-3}$  octanoic acid (a concentration corresponding to a molar ratio of approximately 1:2000 octanoic acid:adipic acid) and  $0.048 \text{ mmol dm}^{-3}$  octanoic acid (1:1400). It im-

mediately became obvious that octanoic acid had a considerable nucleation inhibitory effect, with similarly sized crystals taking an additional 48 h and 168 h to grow in the presence of  $0.034 \text{ mmol dm}^{-3}$  and  $0.048 \text{ mmol dm}^{-3}$  octanoic acid, respectively. Such increases in induction time when growing co-crystals of adipic acid and alcanoic acids have previously been well documented (Davey et al., 1992).

Fig. 8 contains SEM micrographs of crystals grown in the presence of the two concentrations of octanoic acid. As expected, the co-crystals displayed both an elongated morphology about the *b*-axis and pronounced curvature on the crystal faces, whilst the (1 0 0) face maintained its morphological dominance.

AFM imaging in air was performed on the crystals grown in the presence of  $0.034 \text{ mmol dm}^{-3}$  of the inhibitor, and typical images are displayed in Fig. 9. The surface topography appears quite different to that of the un-doped crystals shown in Figs. 3 and 4. The pronounced curvature observed in the SEM micrographs is evident on the individual step edges. Another important observation is the existence of numerous hollow dislocations scattered across the surface of the crystal, which are highlighted with black arrows (Frank, 1951). Hollow cores were not observed on the surface of the un-doped crystals, indicating the possibility of

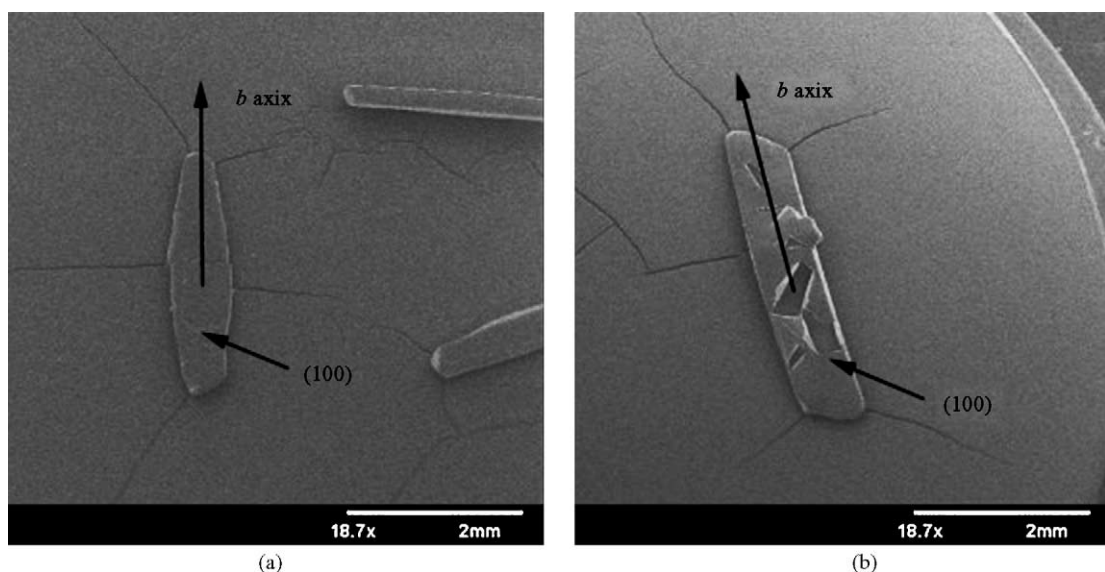


Fig. 8. SEM micrographs of crystals grown in the presence of  $0.034 \text{ mmol dm}^{-3}$  octanoic acid (a) and  $0.048 \text{ mmol dm}^{-3}$  octanoic acid (b). (a and b) 18.7 $\times$  magnification.

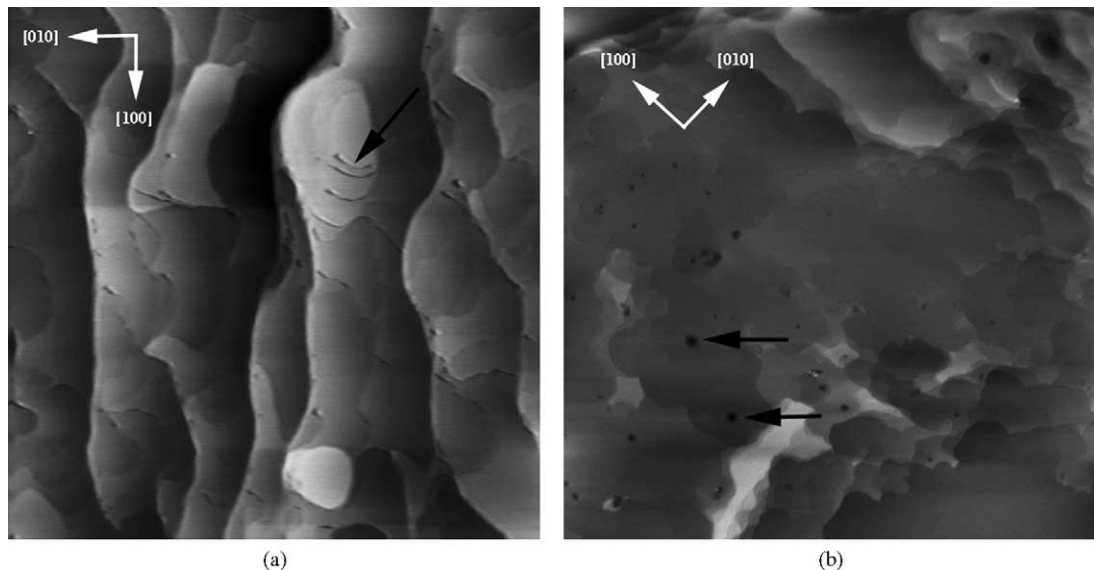


Fig. 9. AFM topographical images of the (100) face of adipic acid crystals grown in the presence of  $0.034 \text{ mmol dm}^{-3}$  octanoic acid. Scan sizes and  $z$ -ranges (a)  $10 \mu\text{m} \times 10 \mu\text{m}$ , 25 nm; and (b)  $13 \mu\text{m} \times 13 \mu\text{m}$ , 100 nm.

increased stress of the dislocations as a consequence of the progressive incorporation of octanoic acid into the crystal lattice throughout growth.

To build up a more thorough picture of the interaction of octanoic acid on crystalline adipic acid, *in situ* AFM imaging was carried out. From experiments carried out in Section 3.2, it was known that imaging solutions in the range  $0.3 < \sigma < 0.4$  were suitable for observing growth on the (100) face of crystalline adipic acid. An un-doped seed crystal was mounted in the AFM, and a solution of  $\sigma = 0.4$  adipic acid was injected into the cell with octanoic acid present at a variety of concentrations.

Low concentrations of octanoic acid had no observable effect on the growth of the (100) surface, with AFM imaging problematic because of growth occurring rapidly, both tangentially and normally to the surface. However, as this concentration was raised, the effect of the impurity started to become clear. Fig. 10a and b shows two consecutive images of the crystal growing in a solution containing  $0.63 \text{ mmol dm}^{-3}$  octanoic acid at  $\sigma = 0.4$  (a concentration corresponding to a molar ratio of approximately 1:350 octanoic acid:adipic acid).

The macrosteps typically observed in the un-doped system (see Fig. 5) appear to have been eradicated,

with single molecular steps now dominating the crystal surface. Some step bunching is apparent; however this is insignificant when compared to the un-doped system. The step edges move noticeably slowly, and dislocations are clearly observable on the crystal surface.

Whilst this level of impurity is not sufficient to completely eradicate tangential growth, it is clear that the octanoic acid is now affecting the development of the (100) surface. The reasons for this are probably two-fold. Firstly, the higher concentrations of impurity may act to lower the system supersaturation slightly—indeed, this would account for the apparent annihilation of the large macrosteps and appearance of screw dislocations on the surface. Secondly, it is possible that the octanoic acid is now at a concentration sufficient to adsorb sporadically to the (100) surface and thus directly interfere with growth, but of insufficient concentration to completely pin the advancing steps.

To investigate this further, the concentration of the guest molecule was doubled to  $1.26 \text{ mmol dm}^{-3}$  (a concentration corresponding to a molar ratio of approximately 1:175 octanoic acid:adipic acid) and numerous images were taken at various points over the whole crystal surface, two of which are displayed

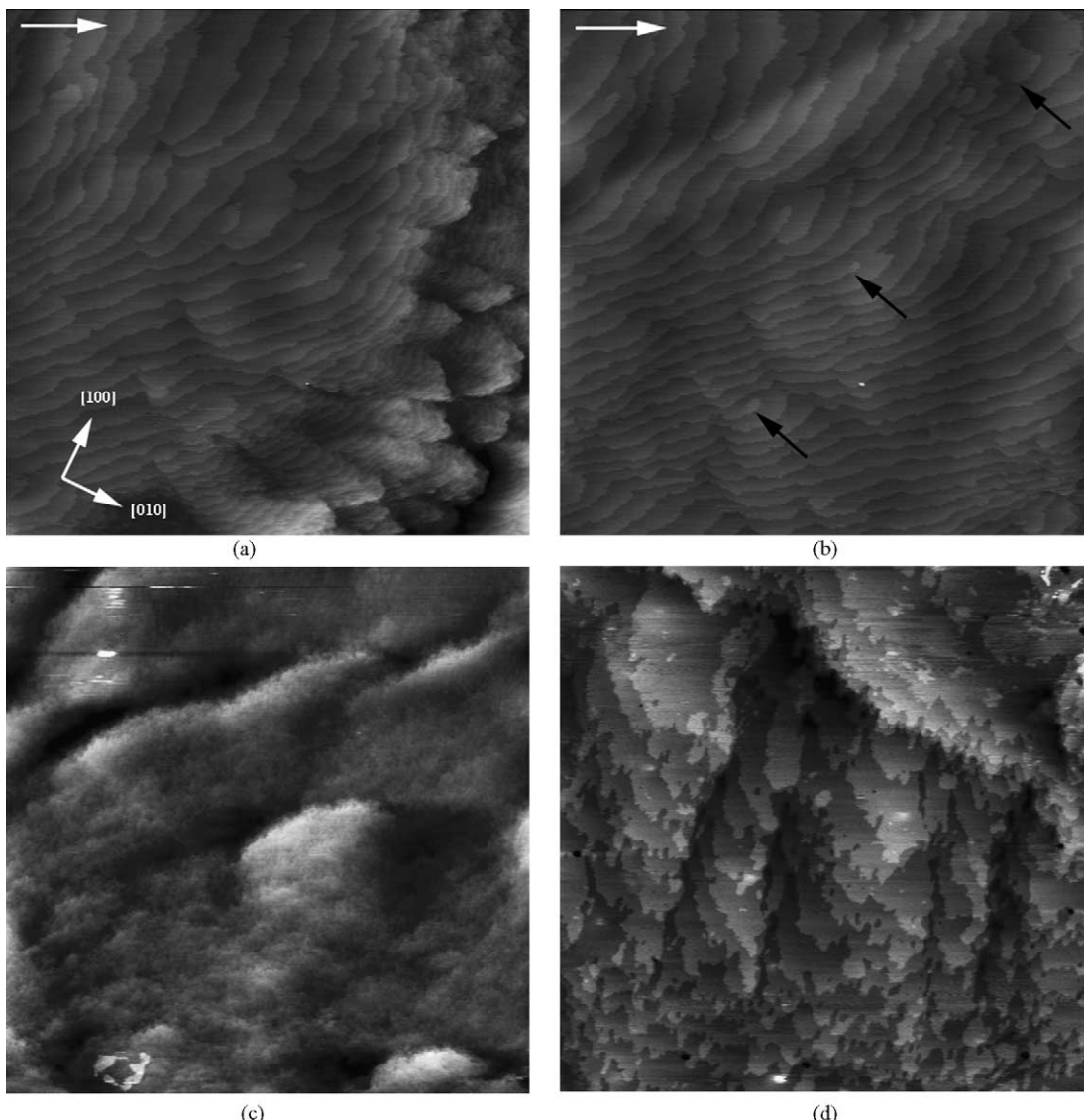


Fig. 10. (a and b) Sequential  $10 \mu\text{m} \times 10 \mu\text{m}$  topographical images of crystalline adipic acid growing in the presence of  $0.63 \text{ mmol dm}^{-3}$  octanoic acid, at a relative supersaturation = 0.4. Growth is occurring from right to left in the images as indicated by the white arrows. Defects are indicated in (b) with black arrows. The  $z$ -range of both (a and b) is 10 nm, with a scan rate of 5.5 Hz. (c and d) Topographical images subsequently captured in the presence of  $1.26 \text{ mmol dm}^{-3}$  octanoic acid, at a supersaturation = 0.4. (c)  $10 \mu\text{m} \times 10 \mu\text{m}$ ,  $z$ -range 20 nm, and (d)  $3 \mu\text{m} \times 3 \mu\text{m}$ ,  $z$ -range 5 nm.

in Fig. 10c and d. The concentration of octanoic acid was now apparently sufficient to inhibit tangential step-wise growth on this face completely, as sequential images displayed negligible signs of growth. Fig. 10d displays a section of the crystal at higher resolution and here the steps appear to be extremely

rough, which is indicative of a high level of incorporation of impurity to the crystal surface.

These observations correlate well with previous modeling and experimental studies. Although it exhibits signs of increased lattice stress, the growth of the (100) face appears to be minimally affected

at low concentrations of the additive. Presumably, this is due to the hydrophilic surface rejecting the comparatively hydrophobic monocarboxylic additive molecules (Williams-Seton et al., 2000), whilst the less hydrophilic faces that bound the (100) face incorporate the additive, thus altering the gross morphology of the crystal. However, as the concentration is raised, it is clear that octanoic acid begins to effect the development of the (100) surface, with growth being inhibited at an additive concentration of  $1.26 \text{ mmol dm}^{-3}$ . This may be due to the binding energy between the octanoic acid molecule and the (100) surface of crystalline adipic acid being significantly larger than that exhibited by the surface and water, ethanol and even adipic acid (Myerson and Jang, 1995). The modeling studies of Myerson and Yang indicate that octanoic acts as a growth inhibitor on this face because of the increased binding that occurs between the (100) surface of adipic acid and octanoic acid. This indeed appears to be the case, but only at elevated concentrations of additive—below this, the (100) face appears to be largely protected by water bound to its hydrophilic surface.

#### 4. Conclusions

The hydrophilic nature of the (100) surface of crystalline adipic acid has long been known to play an important role in determining the gross morphology of the crystal. By utilizing atomic force microscopy (AFM), we have been able to directly observe the (100) face of adipic acid in both air and liquid environments, and in doing so, provide direct microscopic evidence of the importance of hydrophilic nature of this surface.

Firstly, solute reorganization was observed during scanning in air, in both contact and tapping mode. This is a rarely reported phenomenon which, using the force–distance capabilities of AFM, we have investigated and explained as a possible consequence of the hydrophilic nature of the surface permitting local tip-enhanced dissolution and reorganization of the solute. In situ imaging carried out on the seed crystals also revealed the formation of etch pits during dissolution, which can also be attributed to the presence of bound water on the (100) face.

Also presented here are nanoscale observations of the effect of octanoic acid, a structurally-related habit modifier, on the (100) surface of crystalline adipic acid. Initially, doped seed crystals were grown and studied using AFM and SEM. These studies showed that although there seemed to be an increased level of stress within the lattice, the development of the (100) face was apparently unaffected by the presence of relatively low levels of the additive, with the (100) surface retaining its morphological dominance. This observation was confirmed by carrying out in situ experiments, which showed that the presence of low levels of additive had little effect on the development of the (100) surface, presumably because the strongly adsorbed water layer is able to reject the majority of the more hydrophobic alkanoic acid molecules. However, as the concentration of octanoic acid was increased during these in situ experiments, the surface began to exhibit clear changes in step morphology and growth mode. Indeed, at the elevated concentration of  $1.26 \text{ mmol dm}^{-3}$  octanoic acid (a concentration corresponding to a molar ratio of approximately 1:175 octanoic acid:adipic acid), growth on the (100) face was completely inhibited.

#### Acknowledgements

The authors would like to thank the BBSRC for Ph.D. studentship funding for T.R.K. C.T. thanks the EPSRC and GlaxoSmithKline for funding. T.R.K. thanks Dr. C. Gibson and D. Johnson for useful discussions throughout.

#### References

- Cabrera, N., Vermilyea, D.A., 1958. The growth of crystals from solution. In: Turnbull, D. (Ed.), *Growth and Perfection of Crystals*. Wiley, New York, pp. 393–410.
- Cappella, B., Dietler, G., 1999. Force–distance curves by atomic force microscopy. *Surf. Sci. Rep.* 34, 1–104.
- Chan, H.-K., Grant, D.J.W., 1989. Influence of compaction on the intrinsic dissolution rate of modified acetaminophen and adipic acid crystals. *Int. J. Pharm.* 57, 117–124.
- Chow, A.H.-L., Chow, P.K.K., Zhongshan, W., Grant, D.J.W., 1985. Modification of acetaminophen crystals: influence of growth in aqueous solutions containing *p*-acetoxyacetanilide on crystal properties. *Int. J. Pharm.* 24, 239–258.
- Chow, A.H.-L., Grant, D.J.W., 1988a. Modification of acetaminophen crystals. II. Influence of stirring rate during

solution-phase growth on crystal properties in the presence and absence of *p*-acetoxyacetanilide. *Int. J. Pharm.* 41, 29–39.

Chow, A.H.-L., Grant, D.J.W., 1988b. Modification of acetaminophen crystals. III. Influence of initial supersaturation during solution-phase growth on crystal properties in the presence and absence of *p*-acetoxyacetanilide. *Int. J. Pharm.* 42, 123–133.

Chow, K.Y., Go, J., Grant, D.J.W., 1986. Influence of fatty acid additives on the dissolution behavior of adipic acid crystals. *Drug Dev. Ind. Pharm.* 12, 247–264.

Chow, K.Y., Go, J., Mehdizadeh, M., Grant, D.J.W., 1984. Modification of adipic acid crystals: influence of growth in the presence of fatty acid additives on crystal properties. *Int. J. Pharm.* 20, 3–24.

Danesh, A., Connell, S.D., Davies, M.C., Roberts, C.J., Tendler, S.J.B., Williams, P.M., Wilkins, M.J., 2001. An in situ dissolution study of aspirin crystal planes (100) and (001) by atomic force microscopy. *Pharm. Res.* 18, 299–303.

Davey, R.J., Black, S.N., Logan, D., Maginn, S.J., Fairbrother, J.E., Grant, D.J.W., 1992. Structural and kinetic features of crystal growth inhibition: adipic acid growing in the presence of *n*-alkanoic acids. *J. Chem. Soc. Faraday Trans.* 88, 3461–3466.

Davey, R.J., Mullin, J.W., Whiting, M.J.L., 1982. Habit modifications of succinic acid crystals grown from different solvents. *J. Crystal Growth* 58, 304–312.

Davis, A.F., Hadgraft, J., 1991. Effect of supersaturation on membrane transport. 1. Hydrocortisone acetate. *Int. J. Pharm.* 76, 1–8.

Fairbrother, J.E., 1981. Effects of Trace Additives on the Crystal Growth Rate and Habit of a Pharmaceutical Excipient, Adipic Acid. Thesis, University of Nottingham.

Fairbrother, J.E., Grant, D.J.W., 1978. Crystal engineering studies with an excipient material (adipic acid). *J. Pharm. Pharmacol.* 31S, 27P.

Fairbrother, J.E., Grant, D.J.W., 1979. The habit modification of a tablet lubricant, adipic acid. *J. Pharm. Pharmacol.* 30S, 19P.

Florence, A.T., Attwood, D., 1988. *Physicochemical Principles of Pharmacy*. Macmillan Press, Chatham.

Frank, F.C., 1951. Capillary equilibria of dislocated crystals. *Acta Crystallogr.* 4, 497–501.

Garnier, S., Petit, S., Coquerel, G., 2002. Influence of supersaturation and structurally related additives on the crystal growth of alpha-lactose monohydrate. *J. Crystal Growth* 234, 201–219.

Hendriksen, B.A., Grant, D.J.W., 1995. The effect of structurally related substances on the nucleation kinetics of paracetamol (acetaminophen). *J. Crystal Growth* 156, 252–260.

Hendriksen, B.A., Grant, D.J.W., Meenan, P., Green, D.A., 1998. Crystallization of paracetamol (acetaminophen) in the presence of structurally related substances. *J. Crystal Growth* 183, 629–640.

Housty, J., Hospital, M., 1965. Localisation des atomes d'hydrogène dans l'acide adipique COOH[CH<sub>2</sub>]COOH. *Acta Crystallogr.* 18, 693–697.

Jiang, X.N., Sun, D.L., Xu, D., Yuan, D.R., Lu, M.K., Guo, S.Y., Fang, Q., 2001. Investigation of growth modes of cadmium mercury thiocyanate crystal by atomic force microscopy. *J. Crystal Growth* 233, 196–207.

Jiang, X.N., Xu, D., Sun, D.L., Yuan, D.R., Lu, M.K., Guo, S.Y., Zhang, G.H., 2002a. Ex situ atomic force microscopy studies of growth mechanisms of cadmium mercury thiocyanate crystals. *J. Crystal Growth* 234, 480–486.

Jiang, X.N., Xu, D., Yuan, D.R., Sun, D.L., Lu, M.K., Jiang, M.H., 2002b. Atomic force microscopy studies on phase transitions and surface morphology transformation of CMTc crystals. *Appl. Phys. A* 75, 617–620.

Kipp, S., Lacmann, R., Schneeweiss, M.A., 1995. Problems in temperature control performing in situ investigations with the scanning force microscope. *Ultramicroscopy* 57, 333–335.

Li, T., Morris, K.R., Park, K., 2000. Influence of solvent and crystalline supramolecular structure on the formation of etching patterns on acetaminophen single crystals: a study with atomic force microscopy and computer simulation. *J. Phys. Chem. B* 104, 2019–2032.

Michaels, A.S., Colville, A.R., 1960. The effect of surface active agents on crystal growth rate and crystal habit. *J. Phys. Chem.* 63, 13–19.

Michaels, A.S., Tausch, F.W., 1961. Modification of growth rate and habit of adipic acid crystals with surfactants. *J. Phys. Chem.* 64, 1730–1737.

Mullin, J.W., 2001. *Crystallization*. Butterworth-Heinemann, Oxford.

Myerson, A.S., Jang, S.M., 1995. A comparison of binding energy and metastable zone width for adipic acid with various additives. *J. Crystal Growth* 156, 459–466.

Pfefer, G., Boistelle, R., 2000. Theoretical morphology of adipic acid crystals. *J. Crystal Growth* 208, 615–622.

Raghavan, S.L., Trividic, A., Davis, A.F., Hadgraft, J., 2000. Effect of cellulose polymers on supersaturation and in vitro membrane transport of hydrocortisone acetate. *Int. J. Pharm.* 193, 231–237.

Raghavan, S.L., Trividic, A., Davis, A.F., Hadgraft, J., 2001. Crystallization of hydrocortisone acetate: influence of polymers. *Int. J. Pharm.* 212, 213–221.

Shimon, L.J.W., Lahav, M., Leiserowitz, L., 1985. Design of stereoselective etchants for organic crystals. Application for the sorting of enantiomorphs and direct assignment of absolute configuration of chiral molecules. *J. Am. Chem. Soc.* 107, 3375–3377.

Thompson, C., Allen, S., Davies, M.C., Roberts, C.J., Tendler, S.J.B., Wilkins, M.J., Williams, P.M., 2004. The effects of additives on the growth and morphology of paracetamol crystals. *Int. J. Pharm.* 280, 137–150.

Wilkins, S.J., Coles, B.A., Compton, R.G., Cowley, A., 2002. Mechanism and kinetics of salicylic acid dissolution in aqueous solution under defined hydrodynamic conditions via atomic force microscopy: the effects of the ionic additives NaCl, LiCl and MgCl<sub>2</sub>, the organic additives 1-propanol, 2-propanol, and the surfactant sodium dodecyl sulphate. *J. Phys. Chem. B* 106, 4763–4774.

Williams-Seton, L., Davey, R.J., Lieberman, H.F., Pritchard, R.G., 2000. Disorder and twinning in molecular crystals: impurity induced effects in adipic acid. *J. Pharm. Sci.* 89, 346–354.

Zhang, G.G.Z., Grant, D.J.W., 1999. Incorporation mechanism of guest molecules in crystals: solid solution or inclusion? *Int. J. Pharm.* 181, 61–70.